CHEMISTRY
A EUROPEAN JOURNAL

DOI: 10.1002/chem.200501532

Bis-*ortho*-Substitution by Methyl Groups Dramatically Increases the Racemization Barrier of Tröger Bases**

Denis A. Lenev,*[a] Konstantin A. Lyssenko,[b] Denis G. Golovanov,[b] Volker Buss,*[c] and Remir G. Kostyanovsky*[a]

Abstract: We have shown through racemization kinetics studies that the enantiomerization barriers of the bis-*ortho*-methyl substituted Tröger bases **2** and **3** in acidic media are raised by 30 kJ mol^{-1} relative to the parent compound **1**, that is 130.4(4) and 131.6(4) kJ mol^{-1}, respectively (105 °C, pH 1, ethylene glycol). The enantiomerization barrier of *para*-methoxy-*para*-nitro substituted Tröger base **4** was determined by dynamic capillary electrophoresis to 96.3(2) kJ mol^{-1} (25 °C, pH 2.2, H_2O), which is lower by 5 kJ mol^{-1} relative to **1**. The influence of deutero-substitution on the racemization rates was also studied. The influence of steric and electronic factors on the enantiomerization barrier was investigated by quantum-mechanical (DFT) calculations. It is shown that enantiomerization takes place in two steps: ring-opening and further interconversion of the monocyclic intermediate. For the interconversion to occur a transition state has to be passed which is sensitive to steric effects. *Ortho*-substitution by methyl groups significantly increases the energy of this state. Thus, compounds **2** and **3** are the simplest Tröger bases which are configurationally stable in acidic media.

Keywords: chiral resolution · density functional calculations · enantiomerization · nitrogen heterocycles · reaction mechanisms

Introduction

Tröger's base, 2,8-dimethyl-6*H*,12*H*-5,11-methanodibenzo-[*b*,*f*][1,5]diazocine (**1**),[2] is chiral due to two stereogenic nitrogen centers which occupy the bridge head positions of the bicyclic framework and thus are structurally prohibited from inversion. Prelog and Wieland were the first to perform enantioseparation of **1** by chromatography on lactose.[3] The absolute configuration of **1** was determined later[4] from the diastereomeric salt formed with 1,1′-binaphthalene-2,2′-diyl hydrogen phosphate: X-ray diffraction analysis of the crystalline salt unequivocally established the configuration of (+)-**1** as 5*S*,11*S*, in contrast to what had been deduced on the basis of chiroptical evidence.[5] Spurred by the attention that Tröger's base analogues (Tröger bases, TBs) demanded as unique chiral entities their syntheses[6,7] have further been developed and refined. Interest in the chemistry of **1** lies in the realm of asymmetric synthesis, catalysis,[8] and supramolecular chemistry,[4,9] utilizing the concave aromatic scaffold of the base. Particularly noteworthy is the enantioselective DNA intercalation by TBs.[10] Progress in the development of **1** as a versatile chiral tool is been hampered by its stereolability in acidic media.[3,4,11–13] The stereointegrity could be improved,[6d,10b,14] however, the methods tend to ignore[6d,10b] or destroy[14a,b] the geminal methano-bridge. In few cases macrocyclic TB-derived cyclophanes prohibit epimerization,[9b,14c] although this approach lacks generality.

The most probable mechanism for the racemization of TB in acidic media involves formation of the methyleneiminium ion **1a** as a key intermediate (Scheme 1),[11,12] despite the fact that X-ray, NMR- and UV/VIS spectral studies have

[a] Dr. D. A. Lenev, Prof. Dr. R. G. Kostyanovsky
Semenov Institute of Chemical Physics
Russian Academy of Sciences, 4 ul. Kosygina
119991 Moscow (Russia)
Fax: (+7) 495-137-8284
E-mail: lenev@polymer.chph.ras.ru
kost@center.chph.ras.ru

[b] Dr. K. A. Lyssenko, D. G. Golovanov
Nesmeyanov Institute of Organoelement Compounds
Russian Academy of Sciences, 28 ul. Vavilova
119991 Moscow (Russia)

[c] Prof. Dr. V. Buss
Institute of Chemistry, Universität Duisburg-Essen
Lotharstrasse 1, 47048 Duisburg (Germany)
Fax: (+49) 203-379-2772
E-mail: theobuss@uni-duisburg.de

[**] Asymmetric Nitrogen. Part 94; for Part 93 see ref. [1]).

Supporting information for this article is available on the WWW under http://www.chemeurj.org/ or from the author.

failed to provide evidence for such a species.[4,11] For the isomerization reaction to occur the methylene group has to pass through the plane of the benzene ring in order to close the bridge on the opposite side. If this is achieved by rotation about the C4a–N5 bond (or the equivalent C10a–N11 bond) the enantiomerization barrier should increase when the *ortho*-hydrogens at C4 and C10 are substituted by large groups thereby producing strain in the transition state. This rate-decelerating effect might even be enhanced by the supporting role ("buttressing effect"[15]) of a second spacious group in the *meta*-position preventing the outward movement of the *ortho*-substituent.

With these considerations in mind we have synthesized enantiopure **2**, which is the 2,8-desmethyl-4,10-dimethyl isomer of TB **1**, from the dibromo precursor **3**, which forms a racemic conglomerate and undergoes spontaneous resolution by crystallization. Details of the syntheses and the resolution have been described recently.[1] Here we report the barriers to racemization of both **2** and **3** which were determined under acidic conditions and found to be significantly higher than in the parent compound, making them the simplest TBs stable under acidic conditions.

Effects of the deuterium substitution on the racemization rates were studied on enantiopure [D$_6$]-(−)-**1** and [D$_6$]-(−)-**3**. Electronic effects of substitution on the racemization rate were investigated on the example of asymmetrically substituted TB **4**.[16] We also performed quantum-mechanical calculations in order to characterize transition state structures and energy barriers for the enantiomerization of **1** to **4**.

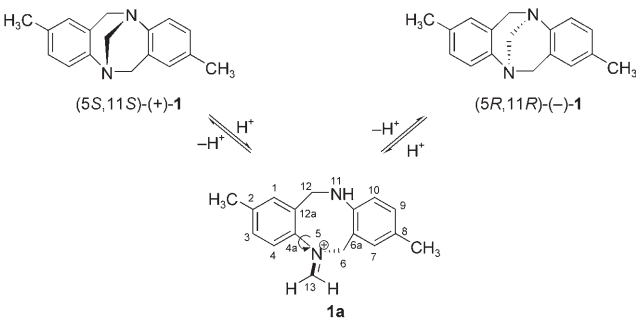

Scheme 1. Formation of the methyleneiminium intermediate during racemization of TB **1**.

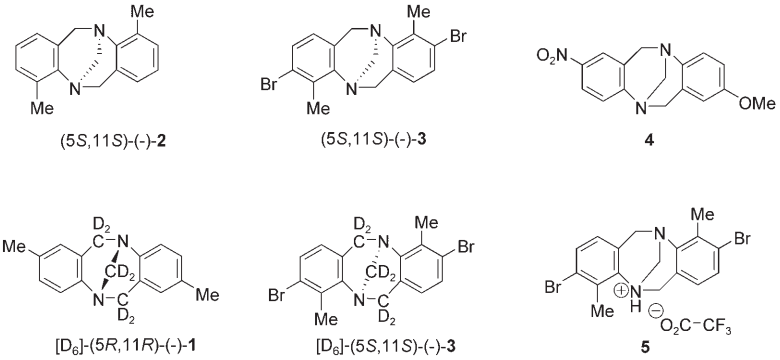

Results and Discussion

Kinetic analyses: Racemization of **1**, [D$_6$]-**1**, **2**, **3** and [D$_6$]-**3** at different temperatures under acidic conditions (0.1 M CF_3SO_3H in ethylene glycol or isobutanol) was followed using either HPLC or circular dichroism (CD) spectroscopical measurements (Tables 1, 2). The pseudo-first order rate constants for racemization k_{rac}, were derived by linear regression of the data according to the first-order kinetic law. Enantiomerization[17] of racemic **4** was studied in aqueous tris-phosphate buffer at pH 2.2 using dynamic capillary electrophoresis (for example, see ref. [12]) with chiral additive

Table 1. Racemization constants and enantiomerization barriers of **1** in 0.1 M CF_3SO_3H/ethylene glycol.

T [°C]	k_{rac} [10^{-5} s^{-1}]	$\Delta G^{\ddagger}_{enant}$ [kJ mol^{-1}]
25.0	2.43(3)[a]	101.0(1)[a]
25.0	3.02(5)	100.5(1)
29.8	5.9(2)	100.5(1)
35.2	12.2(2)	100.4(1)
39.5	20.1(2)	100.6(1)
44.9	38.1(6)	100.7(1)

[a] Values for [D$_6$]-**1**.

Abstract in Russian:

Изучением кинетики рацемизации показано, что барьеры энантиомеризации бис-*орто*-метил замещенных оснований Трёгера **2** и **3** в кислой среде повышаются на 30 кДж моль$^{-1}$, по сравнению с родоначальным соединением **1**, и составляют 130.4(4) и 131.6(4) кДж моль$^{-1}$ (105 °C, pH 1, этиленгликоль). Барьер энантиомеризации *пара*-метокси-*пара*-нитро замещенного основания Трёгера **4**, найденный методом динамического капиллярного электрофореза, составляет 96.3(2) кДж моль$^{-1}$ (25 °C, pH 2.2, H_2O), что ниже на 5 кДж моль$^{-1}$ по сравнению с **1**. Изучено влияние дейтеро-замещения на скорость рацемизации. Влияние стерических и электронных факторов на барьер энантиомеризации исследовано квантовомеханическими (DFT) расчетами. Показано, что энантиомеризация протекает в две стадии: раскрытие бицикла и интерконверсия моноциклического интермедиата. В процессе интерконверсии образуется переходное состояние, чувствительное к стерическим эффектам. *Орто*-замещение метильными группами значительно увеличивает энергию этого состояния. Т.о. соединения **2** и **3** являются простейшими основаниями Трёгера, конфигурационно устойчивыми в кислой среде.

Table 2. Racemization constants and enantiomerization barriers of **2** and **3**.

T [°C]	k_{rac} [10^{-5} s^{-1}] (**2**)	$\Delta G^{\neq}_{enant}$ (**2**) [kJ mol^{-1}]	k_{rac} [10^{-5} s^{-1}] (**3**)	$\Delta G^{\neq}_{enant}$ (**3**) [kJ mol^{-1}]
100[a]	1.01(2)	129.9(3)	0.517(3)	131.9(4)
100[b]	0.89(1)	130.3(4)	–	–
105[b]	1.49(6)	130.4(4)	1.03(9)	131.6(4)
110[b]	2.1(1)	131.1(4)	1.6(1)	132.0(4)
115[b]	3.3(2)	131.4(4)	2.5(2)	132.3(4)
120[b]	5.3(1)	131.6(4)	3.64(3)	132.8(4)
120[b,c]			4.17(6)	132.4(4)

[a] 0.1 M CF_3SO_3H/Me_2CHCH_2OH. [b] 0.1 M CF_3SO_3H/ethylene glycol. [c] Values for [D_6]-**3**.

2-hydroxypropyl-β-cyclodextrin (Table 3). The rate constants k_{enant} for enantiomerization of **4** were derived from chromatographic parameters by using recently developed unified

Table 3. Enantiomerization constants and enantiomerization barriers of **4** at pH 2.2 in 50 mM tris-phosphate buffer.

T [°C]	k_{enant} [10^{-5} s^{-1}]	$\Delta G^{\neq}_{enant}$ [kJ mol^{-1}]
20	4.89	96.0(3)
25	8.47	96.3(2)
30	16.1	96.3(2)
35	31.5	96.22(2)
40	66.8	95.9(3)

equation for dynamic chromatography, implemented in the DCXplorer software.[18] From the k_{rac} or k_{enant} values the free energy barriers to enantiomerization, $\Delta G^{\neq}_{enant}$, were calculated using the Eyring Equations (1) and (2) where κ is the statistical transmission factor (set equal to 1, see calculations below). The influence of the protonation–deprotonation equilibrium (Scheme 2) on the racemization kinetics and the selection of the pH value for the measurements

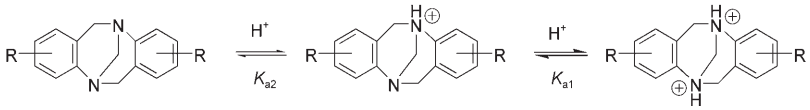

Scheme 2. Protonation–deprotonation equilibrium for TBs.

were considered based on the data reported previously. Thus, the pK_{a2} of **1** is 3.2,[19] whereas its pK_{a1} is ≈0.[11] We therefore conclude that at pH 1 compounds **1** to **3** are present mainly in the monocationic form. Probably, at pH 2.2 the compound **4** is also mainly monoprotonated. This assumption allowed us to use pseudo-first order constants instead of complete ones. An additional kinetic experiment performed at 120 °C with a twofold increase of the acid concentration (0.2 M) and otherwise identical conditions showed that the rate constant for racemization of **3** decreased by 12 %. This effect can be rationalized by increase of the concentration of the dication, which is stereochemically the more stable species.

$$k_{enant} = \kappa(k_B T h^{-1}) e^{\frac{-\Delta G^{\neq}}{RT}} \quad (1)$$

$$k_{rac} = 2k_{enant} \quad (2)$$

From Eyring plots of $\ln(k_{enant}/T)$ versus $1/T$ (Figures 1–4) the activation parameters of enantiomerization $\Delta H^{\neq}_{enant}$ and $\Delta S^{\neq}_{enant}$ for compounds **1** to **4** were obtained (Table 4). They

Table 4. Experimental activation parameters to enantiomerization and calculated transition state energies for compounds **1** to **4**.

	$\Delta H^{\neq}_{enant}$ [kJ mol^{-1}]	$\Delta S^{\neq}_{enant}$ [J mol^{-1} K^{-1}]	$\Delta G^{\neq}_{enant}$ (105 °C) [kJ mol^{-1}]	k_{enant} (105 °C) [s^{-1}]	E(TS2) [kJ mol^{-1}][b]
1	98(1)	−9(4)	101(2)[a]	0.03–0.21[a]	84.4
2	103(3)	−73(8)	130.4(4)	1.49×10^{-5}	121.0
3	101(2)	−81(6)	131.6(4)	1.03×10^{-5}	128.9
4	98(3)	6(10)	96(7)[a]	0.05–4[a]	65.3

[a] Extrapolated values. [b] Calculated (using density functional theory) energies of the transition states TS2 (see below).

were used to extrapolate linearly the rate constants for the compounds **1** and **4** to higher temperatures and for the compounds **2** and **3** to lower temperatures. We note a) that the barrier to enantiomerization for **1** is very close to the previously reported value (100.9 kJ mol^{-1} at 25 °C, pH 2.2, H_2O[12]), b) that asymmetric *para*-nitro, *para*-methoxy substitution in **4** decreases the barrier by ~5 kJ mol^{-1} and c) that *ortho*-methyl substitution increases the barrier by ~30 kJ mol^{-1}. Thus, at 105 °C, k_{enant}(**1**)/k_{enant}(**3**) > k_{enant}(**1**)/k_{enant}(**2**) > 2000, which indicates the significant decrease in reactivity of **2** and **3**. There is a small effect of the additional *meta*-Br substituent, which lowers the corresponding rate constant by a factor of ≈1.5 and raises the enantiomerization barrier by 1 kJ mol^{-1} (Table 4). Isotopic effects of deuterium were also observed. Thus, compound [D_6]-**1** racemizes slower, than the protonated analogue with k_{rac}(**1**)/k_{rac}([D_6]-**1**$_6$) = 1.24, whereas the opposite trend is observed for **3**: k_{rac}(**3**)/k_{rac}([D_6]-**3**) = 0.87. This could be rationalized by increased effective steric volume of H in comparison to D, leading to retardation of racemization in the sterically hindered proto-**3**. Table 5 summarizes calculated half-times for racemization of the compounds **1** to **4** at different temperatures and pH. Figure 5 exemplifies plateau formation between two peaks of interconverting enantiomers of **4** in a typical electropherogram at 40 °C.

Calculations and structure: To model the enantiomerization reaction we have examined possible enantiomerization pathways of the protonated TB with density functional theory (B3LYP at the 6-31G(d,p) level). In particular, we studied intermediates and transition states of **3**, supplemented by se-

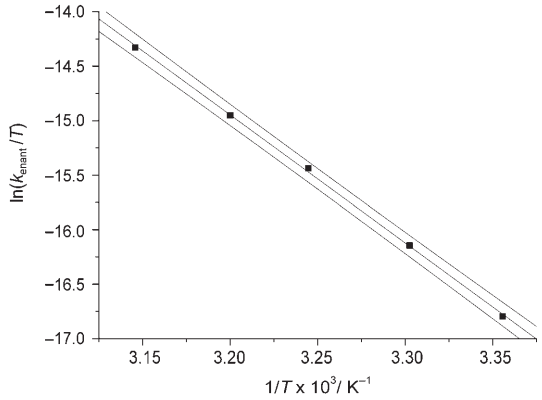

Figure 1. Eyring plot for the determination of the activation parameters of **1** from the kinetic experiments, the upper and lower lines represent the error bands of the linear regression with a 95% confidence level. The correlation coefficient R is 0.9997.

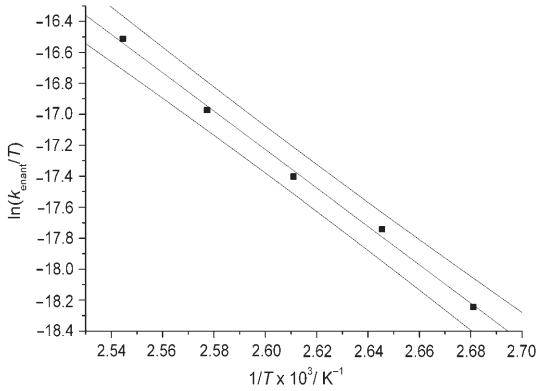

Figure 2. Eyring plot for the determination of the activation parameters of **2** from the kinetic experiments; $R=0.998$.

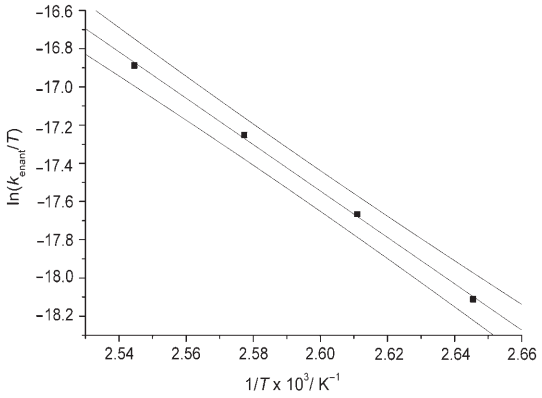

Figure 3. Eyring plot for the determination of the activation parameters of **3** from the kinetic experiments; $R=0.9994$.

lected structures of **1** and **2**. The (*R*,*R*)-configured bicyclic structure of protonated **3** was optimized starting with the crystal structure of the racemic monotrifluoroacetate **5** (Figure 6). In agreement with the X-ray data, and typical for protonated Tröger bases,[20] the bridging methylene group is significantly displaced towards the unprotonated nitrogen in

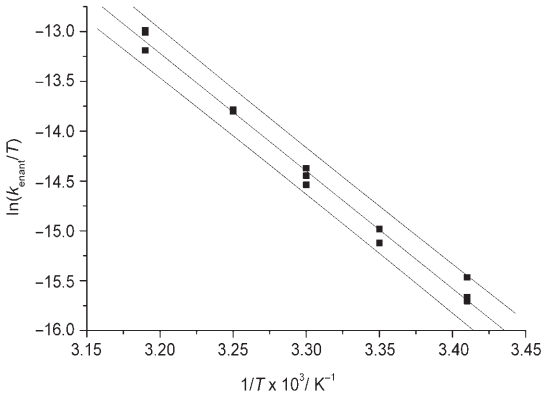

Figure 4. Eyring plot for the determination of activation parameters for racemization of **4** from the calculated rate constants; $R=0.994$.

Table 5. Racemization half-times for compounds **1** to **4** at different temperatures and pH.

T [°C]	pH	**1**	**2**	**3**	**4**
105	1	2–10 s[a]	12.9 h	18.7 h	0.1–7 s[a]
105	7[b]	3–15 h	9.6 y	13.4 y	0.2–12 h
25	1	6.4 h	13 y[a]	15 y[a]	1.1 h
25	7[b]	4.6 y	10^5 y	10^5 y	1 y

[a] Extrapolated values. [b] Calculated values, assuming pK_{a2} 3.2.

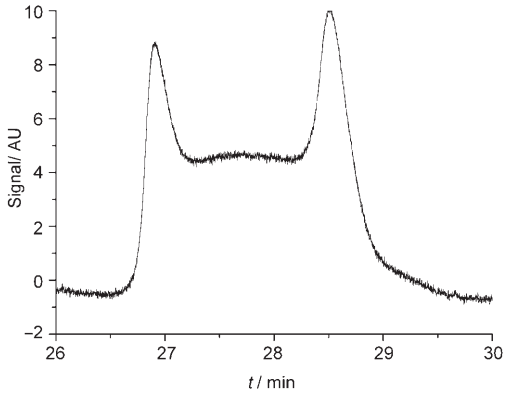

Figure 5. Plateau formation between the peaks of two interconverting enantiomers in a typical electropherogramm of **4** (40°C, pH 2.2, 50 mM tris-phosphate buffer, 20 mM 2-hydroxypropyl-β-cyclodextrin).

anticipation of the ring-opening step. Actual ring opening requires 71.4 kJ mol^{-1} (see Figure 7) and leads to the first monocyclic intermediate. The conformational behaviour of similar substituted eight-membered rings including their inversion which is a requirement for enantiomerization of **3** has been extensively studied previously.[21] In short, there should exist at least four enantiomeric pairs of stable conformations (one chair, two folded and one extended twist-boat form) and seven pairs of transition states for their interconversion. Several of these structures have been found and characterized as stationary points on the potential energy landscape; they are shown schematically in Figure 7. The high energies of these conformations correlate with the high

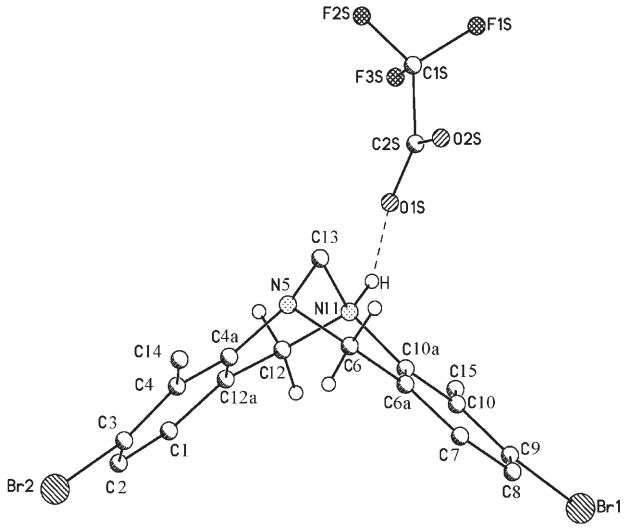

Figure 6. Projection of the molecular structure of the compound **5** in the solid state.

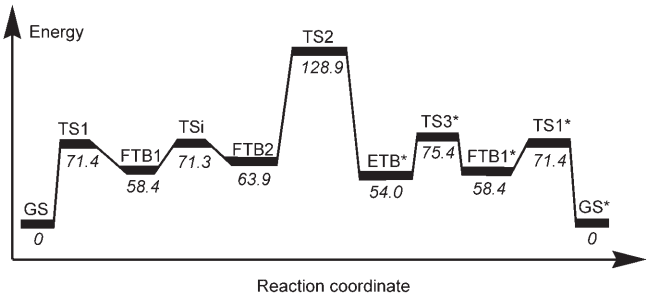

Figure 7. DFT-calculated stationary points for protonated **3** and possible pathway for enantiomerization. Asterisks indicate positive values for the dihedral angle C4-C4a-N5-C13 (see text). Energies (in italics; in kJ mol^{-1}) relative to the (*R*,*R*)- and (*S*,*S*)-bicyclic structures, GS and GS*, respectively. FTB1 and FTB2 are folded twist-boat and ETB extended twist-boat conformations; TS1 to TS3 and TSi represent transition states.

electrophilicity of isolated methyleneiminium salts,[22] which is why they are present in only negligible amounts in the reaction mixtures.[11] However, of the multitude of structures only a few are relevant with respect to the inversion process.

According to our hypothesis it is the rotation of the $N^+=CH_2$ group through the plane of the aromatic ring which defines the reaction progress. Therefore, the structures can be divided into two groups according to the position of the methylene group ("above" or "below") relative to this plane which makes the dihedral angle C4-C4a-N5-C13 the "indicator of chirality". Most important are therefore transition state(s) which connect structures of opposite chirality. Using the STQN algorithm[23] we could locate only one such structure (TS2 in Figure 7) which connects a folded twist-boat conformation (FTB2) with the inverted extended twist-boat conformation ETB*.

The structure of TS2 is shown in Figure 8. Its most prominent feature is the heavy puckering of the aromatic ring ex-

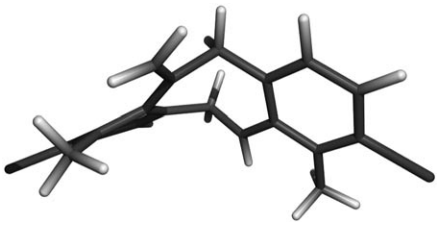

Figure 8. Stick model of the transition state (TS2) for enantiomerization of protonated **3**. The view is approximately along the C6–C12 axis; the $N^+=CH_2$ group is in the front. Note the bent *ortho*-methyl group.

emplified by the dihedral angle C3-C4-C4a-C12a which is −15.6°. This non-planar deformation is caused by the strong steric repulsion between the methylene group and the methyl group in the *ortho*-position which is clearly visible in the Figure. In the corresponding transition state of **2** the strain is lower leading to a pucker angle (as defined above) of only −8.7°. Finally, in **1** and **4** the benzene ring remains essentially planar during the interconversion. Independent of the substitution the transition state is chiral; therefore the equivalent back reaction must pass through the enantiomeric transition state TS2*. The two equivalent transition states TS2 and TS2* and two equivalent protonation sites in the molecule bring the value of the statistical transmission factor κ in the Eyring Equation (1) to unity (see above).

The calculated energies of the three transition states are shown in Table 4 next to the experimentally determined free energies of enantiomerization. The agreement is satisfactory for **2** and for **3**; also, the significantly lower barrier of **1** is correctly reproduced. The asymmetric substitution of **4**, from general considerations, should lead to stabilization of the transition state TS2 by π-conjugation. Indeed, the calculated value of the energy of TS2 for **4** is 65.3 kJ mol^{-1}. The observed modest lowering of the barrier from 101 to 96 kJ mol^{-1} might be explained by the fact that the Figure 7 in general is no longer true for **4**: the TS2 is probably not the most energetic transition state and rate is determined by other transition states in the Figure. Another important message is that the negative activation entropy for racemization of **2** and **3** (Table 4) might show the significant role of the solvation effects in the activated complexes (cf. ref. [24]), which should be the subject of further investigations.

In summary we have shown that bis-*ortho* substitution by methyl groups raises the barrier to enantiomerization of Tröger bases, dramatically enhancing their configurational stability in acidic media. According to quantum-mechanical calculations inversion takes place in two steps. Protonation initiates the ring-opening step and formation of the first iminium ion which equilibrates via relatively low lying transition states with other conformers. For enantiomerization to occur a transition state has to be passed which appears to be highly sensitive to steric effects. Our calculations show that *ortho* substitution by methyl groups increases significantly the energy of this state and thus is able to cause the observed configurational stability.

Configurationally stable Tröger bases may be used in asymmetric aminomethylation, other acid- or non-nucleophilic base-promoted enantioselective reactions, and for molecular recognition in a broad pH range. As has been pointed out[6b] *ortho*-substituents increase the volume of the hydrophobic pocket in TBs, which along with the present findings strongly enhances the supramolecular potential of the system.

Experimental Section

General methods: Triflic and trifluoroacetic acids (puriss.) were purchased from Fluka and used without purification. [D_2]Paraformaldehyde (99% D) was purchased from Acros. Ethylene glycol and isobutanol were distilled from CaH_2.

[D_6]-(±)-**1**: Synthesized according to described procedure, with $(CD_2O)_n$ used as formaldehyde equivalent.[6e] M.p. 137°C; ^{1}H NMR (400 MHz, $CDCl_3$): δ = 2.10 (s, 6H, 2Me), 6.59 (d, 2H, ^4J = −1.5 Hz), 6.85 (dd, 2H, ^3J = 8.1, ^4J = −1.5 Hz), 6.92 (d, 2H, ^3J = 8.1 Hz); ^{13}C NMR (100 MHz, $CDCl_3$): δ = 23.0 (Me), 60.3 (quint, $ArCD_2N$, $^1J_{CD}$ = 20 Hz), 68.2 (m, NCD_2N, $^1J_{CD}$ = 20 Hz), 126.9, 129.4, 129.5, 130.3, 135.5, 147.6; ESI-MS: *m*/*z*: calcd for $C_{17}H_{13}D_6N_2$: 257.19187; found: 257.19185 $[M+H]^+$.

[D_6]-(±)-**3**: Synthesized according to described procedure with $(CD_2O)_n$ used as formaldehyde equivalent.[6a] M.p. 220–222°C; ^{1}H NMR (400 MHz, $CDCl_3$): δ = 2.39 (s, 2Me, 6H), 6.56 (d, 2H, ^3J = 8 Hz), 7.14 (d, 2H, ^3J = 8 Hz); ^{13}C NMR (100 MHz, $CDCl_3$): δ = 17.7, 54.6 (quint, $ArCD_2N$, $^1J_{CD}$ = 20 Hz), 66.9, (m, NCD_2N, $^1J_{CD}$ = 20 Hz), 124.5, 125.9, 127.2, 128.3, 133.4, 147.6; ESI-MS: *m*/*z*: calcd for $C_{17}H_{11}D_6Br_2N_2$: 413.01296; found: 413.01287 $[M+H]^+$.

3,9-Dibromo-4,10-dimethyl-6*H*,12*H*-5,11-methano-dibenzo[*b*,*f*]-[1,5]diazocinium trifluoroacetate (5): The title compound was obtained by slow evaporation of the diluted solution of **3** in 0.1 M CF_3COOD/CD_2Cl_2 to yield transparent plates. M.p. 160°C (gas evolution); ^{1}H NMR (400 MHz, CD_2Cl_2): δ = 2.53 (s, 6H, 2Me), 4.03 (d, ^2J = −17 Hz, 2H, CH_aAr), 4.58 (s, NCH_2N), 4.77 (d, ^2J = −17 Hz, 2H, CH_bAr), 6.77 (d, ^3J = 8 Hz, 2H), 7.23 (br s, 1H, NH), 7.37 (d, ^3J = 8 Hz, 2H).

At 120 K crystals of **5** are monoclinic, space group $P2_1/n$, a = 7.3751(7), b = 17.803(2), c = 14.373(1) Å, β = 99.087(2), V = 1863.5(3) Å^3, Z = 4, ρ_{calcd} = 1.861 g cm^{-3}. Intensities of 19107 reflections were measured with a SMART 1000 CCD diffractometer ($\lambda(Mo_{K\alpha})$ = 0.71072 Å, $2\theta < 56°$), and 4491 independent reflections (R_{int} = 0.0302) were used in further refinement. The refinement converged to wR_2 = 0.0610 and GOF = 1.086 for all independent reflections ($R1$ = 0.0281 was calculated against F for 3614 observed reflections with $I > 2\sigma(I)$). All calculations were performed using SHELXTL PLUS 5.1.

CCDC-232751 contains the supplementary crystallographic data for this paper. These data can be obtained free of charge from The Cambridge Crystallographic Data Centre via www.ccdc.cam.ac.uk/data_request/cif.

Enantiopure 1 and [D_6]-**1** were prepared according to ref. [4], enantiopure **2**, **3**, and [D_6]-**3** according to refs. [1,6a], racemic **4**, according to ref. [16].

Kinetic experiments for **1** to **3** were performed in solution in glass vials in thermostated oil baths. In each of the series, the free base was dissolved in CF_3COOH, and the excessive acid was rapidly removed under reduced pressure at room temperature. The residue was then dissolved in acidic ethylene glycol (typical concentration 5×10^{-3} M) and the solution divided into aliquots, which were immersed in the thermostat. For compound **1**, at each time point the vial contents were neutralized with aqueous NH_3, extracted with hexane and analyzed by HPLC on a chiral stationary phase Whelk R,R O 1, hexane/EtOH 98:2 as a mobile phase with UV detection at 254 nm; the retention times of the enantiomers were 9.1 min for (+)-**1** and 9.9 min for (−)-**1**. System was equipped with Shimadzu C-R3A integrator. For compounds **2** and **3**, the vials were cooled by liquid nitrogen, brought to room temperature, and the contents were analyzed using the decay of the CD signal at 265 nm. For each temperature, the rate constants were obtained by linear regression of the data to the first-order kinetics law (six data points). For CD measurements, maximal values of CD signal (ΔA) at each point of time (t) were taken, divided by the value of ΔA at t = 0 (ΔA_0), and logarithm of the ratio $\ln(\Delta A_0/\Delta A)$ was plotted against t. The slope constituted the pseudo first-order rate constant k_{rac} (see Supporting Information). For HPLC measurements, the integration values were used to calculate enantiomeric excess (ee), and $\ln(ee_0/ee)$ was plotted against t. Again, the slope constituted the first-order rate constant k_{rac}. The chemical integrity of the samples after racemization was monitored and confirmed by HPLC, UV and NMR.

Dynamic capillary electrophoresis for **4** was performed using Agilent ^{3D}CE system (Agilent, Waldbronn, Germany), equipped with a diode array detector (DAD). Fused silica capillary with dimensions of 50 μm i.d. × 60 cm (51.5 cm effective length) was thermostated by air. The experiments were performed applying 30 kV voltage, in tris-phosphate buffer (50 mM) at pH 2.2 with 2-hydroxypropyl-β-cyclodextrin (20 mM) as a chiral additive. Sample solution of **4** in the buffer (1 mg mL^{-1}) was injected by applying pressure of 50 mbar for 5 s. The analyte was detected by DAD at 220 ± 20 nm.

Computations were performed in the computing center of Cologne University (RRZK) using Gaussian 03, Revision B.04, Gaussian, Inc., Pittsburgh PA, 2003. The crystal structure of **5** was taken as a starting point for the geometry optimizations. Preliminary calculations were run at the AM1 level, and the minima search starting from the transition states was done using the Intrinsic Reaction Coordinate (IRC) routine implemented in the package.[23] Thus, using both IRC and STQN,[23] the full reaction path for **5** was calculated, and the AM1 structures were then used as guesses for the high level DFT geometry optimizations. Each structure at DFT level was characterized by frequency calculation, local minima having no and transition states one imaginary frequency.

Acknowledgements

This work was supported by the Russian Foundation for Basic Research (grant Nos. 03-03-32019 and 03-03-04010), the Russian Academy of Sciences (Nefedov–Tartakovsky programmes) and INTAS (grant No. YS 04-83-3442). We thank Dr. I. Vystorop, Dr. K. Kaval, Prof. Dr. V. Schurig, P. A. Levkin and Prof. Dr. M. Maier for helpful discussions and assistance. Special thanks to Dr. O. Trapp for calculation of the rate constants for the compound **4** and Dr. D. Wistuba for performing capillary electrophoresis experiments.

[1] D. A. Lenev, K. A. Lyssenko, D. G. Golovanov, O. R. Malyshev, P. A. Levkin, R. G. Kostyanovsky, *Tetrahedron Lett.* **2006**, *47*, 319–321.
[2] J. Tröger, *J. Prakt. Chem.* **1887**, *36*, 225–245.
[3] V. Prelog, P. Wieland, *Helv. Chim. Acta* **1944**, *27*, 1127–1134.
[4] S. H. Wilen, J. Z. Qi, P. G. Williard, *J. Org. Chem.* **1991**, *56*, 485–487.
[5] a) O. Cervinka, A. Fabryova, V. Novak, *Tetrahedron Lett.* **1966**, 5375–5377; b) S. F. Mason, K. Schofield, R. J. Wells, J. S. Whitehurst, G. W. Vane, *Tetrahedron Lett.* **1967**, 137–141.
[6] a) A. Hansson, J. Jensen, O. F. Wendt, K. Wärnmark, *Eur. J. Org. Chem.* **2003**, 3179–3188; b) J. Jensen, M. Strozyk, K. Wärnmark, *Synthesis* **2002**, 2761–2765; c) F. Salort, C. Pardo, J. Elguero, *Magn. Reson. Chem.* **2002**, *40*, 743–746; d) A. Tatibouët, M. Demeunynck, H. Salez, R. Arnaud, J. Lhomme, C. Courseille, *Bull. Soc. Chim. Fr.* **1997**, *134*, 495–501; e) M. Häring, *Helv. Chim. Acta* **1963**, *46*, 2970–2982.
[7] a) B. Cekavicus, E. Liepinsh, B. Vigante, A. Sobolevs, J. Ozols, G. Duburs, *Tetrahedron Lett.* **2001**, *42*, 4239–4241; b) R. Abonia, E. Rengifo, J. Quiroga, B. Insuasty, A. Sanchez, J. Cobo, J. Low, M. Nogueras, *Tetrahedron Lett.* **2002**, *43*, 5617–5620.

[8] a) S. Sergeyev, F. Diederich, *Angew. Chem.* **2004**, *116*, 1770–1773; *Angew. Chem. Int. Ed.* **2004**, *43*, 1738–1740; b) M. Harmata, M. Kahraman, *Tetrahedron: Asymmetry* **2000**, *11*, 2875–2879.
[9] a) A. Manjula, M. Nagarajan, *Tetrahedron* **1997**, *53*, 11859–11868; b) T. H. Webb, H. Suh, C. S. Wilcox, *J. Am. Chem. Soc.* **1991**, *113*, 8554–8555; c) M. J. Crossley, T. W. Hambley, L. G. Mackay, A. C. Try, R. Walton, *J. Chem. Soc. Chem. Commun.* **1995**, 1077–1079.
[10] a) E. Yashima, M. Akashi, N. Miyauchi, *Chem. Lett.* **1991**, 1017–1020; b) A. Tatibouët, M. Demeunynck, C. Andraud, A. Collet, J. Lhomme, *Chem. Commun.* **1999**, 161–162.
[11] A. Greenberg, N. Molinaro, M. Lang, *J. Org. Chem.* **1984**, *49*, 1127–1130.
[12] O. Trapp, G. Trapp, J. Kong, U. Hahn, F. Vögtle, V. Schurig, *Chem. Eur. J.* **2002**, *8*, 3629–3634.
[13] R. G. Kostyanovsky, V. R. Kostyanovsky, G. K. Kadorkina, K. A. Lyssenko, *Mendeleev Commun.* **2003**, 111–113.
[14] a) Y. Hamada, S. Mukai, *Tetrahedron: Asymmetry* **1996**, *7*, 2671–2674; b) Y. Miyahara, K. Izumi, A. A. Ibrahim, T. Inazu, *Tetrahedron Lett.* **1999**, *40*, 1705–1708; c) U. Maitra, B. G. Bag, P. Rao, D. Powell, *J. Chem. Soc. Perkin Trans. 1* **1995**, 2049–2056.
[15] E. L. Eliel, S. H. Wilen, *Stereochemistry of organic compounds*, Wiley, New York, **1994**, p. 1144.
[16] C. Pardo, M. Ramos, A. Fruchier, J. Elguero, *Magn. Reson. Chem.* **1996**, *34*, 708–710.
[17] C. Wolf, *Chem. Soc. Rev.* **2005**, *34*, 595–608.
[18] O. Trapp, *Anal. Chem.* **2006**, *78*, 189–198.
[19] B. M. Wepster, *Recl. Trav.Chim. Pays-Bas* **1953**, *72*, 661–672.
[20] D. A. Lenev, K. A. Lyssenko, R. G. Kostyanovsky, *Russ. Chem. Bull.* **2000**, *49*, 1241–1244; *Izv. Akad. Nauk. Ser. Khim.* **2000**, 1244–1247 (in Russian).
[21] R. Crossley, A. P. Downing, M. Nogradi, A. Braga de Oliveira, W. D. Ollis, I. O. Sutherland, *J. Chem. Soc. Perkin Trans. 1* **1973**, 205–217.
[22] *Iminium salts in organic chemistry* (Eds.: H. Böhme, H. G. Viehe), Wiley, New York, **1976**.
[23] J. B. Foresman, Æ. Frisch, *Exploring Chemistry with Electronic Structure Methods*, 2nd ed., Gaussian, Inc., Pittsburgh, PA, **1996**.
[24] R. Meissner, X. Garcias, S. Mecozzi, J. Rebek Jr., *J. Am. Chem. Soc.* **1997**, *119*, 77–85.

Received: December 7, 2005
Revised: February 3, 2006
Published online: May 26, 2006

